# Supporting Information

## Electrical Textile Valves for Paper Microfluidics

*Alar Ainla, Mahiar M. Hamedi, Firat Güder and George M. Whitesides**

## Currently existing valve technologies for paper devices

**Table S1.** Summary of flow-control and valve technologies relevant for paper microfluidic devices. The table includes currently reported paper valves, as well as other methods to regulate flows in paper microfludics, and valves which have been reported for other types of microfluidics, but could be relevant also in the context of paper devices. We divide devices by their type into chemical (Chem.) and physical (Phys.), where chemical devices operate based on changes in chemical composition (reaction or dissolution), while physical devices do not involve such changes. Physical devices are less likely to interfere with assays, since no additional compounds are released during the actuation of these valves.

| Reference | General description | Actuated by/ Normal state/ Operation mode | Type | Flow control is used during / repeatability | *Pros* | *Cons* |
|---|---|---|---|---|---|---|
| **Valves for wicking-based paper microfluidic devices** | | | | | | |
| Y. Jiang, Z. Hao, Q. He and H. Chen, *RSC Adv.*, 2016, **6**, 2888–2894. | Liquid impermeable hydrophobic barrier is treated with hand-held corona generator, which renders it hydrophilic and liquid permeable (opening is fast, within 1s). | Electric plasma / Closed / Discrete opening | Chem | Operation / One time | Simple low-cost paper device. No moving parts. Electrical control. Fast to open (in 1s). | Corona generator is expensive (>500USD). Electromagnetic noise (10-45kV, 4.5MHZ). Safety concerns. Large energy consumption (40W). Plasma may damage sample. |

| | | | | | | |
|---|---|---|---|---|---|---|
| C. K. W. Koo, F. He and S. R. Nugen, *Analyst*, 2013, **138**, 4998–5004. | Electrchemical valves containing printed conductive paper (reactive silver ink), which is treated with hydrophobic thiol. This barrier is not wicked by liquid readily (though not completely impermeable), but when low voltage (4V or above) is applied, it erodes the thiol and wicking speed increases (about 10x). | Electrical signal / Closed / Wicking speed modulation | Chem | Operation / On time | Simple low-cost device. No moving parts. Simple low-voltage electrical control. | Electrochemical reaction may damage sample/reagents. Relatively slow (100s). No complete closure. |
| P. Zwanenburg, X. Li and X. Y. Liu, *Proc. IEEE Int. Conf. Micro Electro Mech. Syst.*, 2013, 253–256. | Magnetic valve based on paper cantilever containing magnetic PDMS. This cantilever can move and can connect or disconnect the paper channel. Cantilever is moved by an electromagnet . | Electro-magnet / Either Closed or Open / Discrete switching | Phys | Operation / Reversible | Fast switching. Electrical control. Reversible. No chemical interference. | Mechanically moving parts and complicated device design. Electromagnets are quite large. |
| M. M. Hamedi, V. E. Campbell, P. Rothemund, F. Güder, D. C. Christodoulou, J.-F. Bloch and G. M. Whitesides, *Adv. Funct. Mater.*, 2016, n/a–n/a. | Electrically activated paper actuator, which bends. This cantilever can be used to connect and disconnect paper channel to and from the liquid. Principle of the actuator is based on reversible expansion and contraction of cellulose, when adsorbing water from air. Adsorption is further controlled by electrical heating with PEDOT:PSS heaters made into same paper device. | Electrical heating / Either Closed or Open / Discrete switching | Phys | Operation / Reversible | Low-cost device. Reversible. Simple electrical control. | Mechanically moving parts. High voltage (100V) / power required to heat. Relatively slow 15-20s. High temperature may affect the assay. Actuation depends on the surrounding humidity. |
| Y. Matsuda, S. Shibayama, K. Uete, H. Yamaguchi and T. Niimi, *Anal. Chem.*, 2015, 1–8. | Electrical heater is used to evaporate liquid, which effectively stops the wicking of liquid front. Heater is printed to the paper using low-resistance silver nanoparticle ink. Valve operates in the range of 10s. | Heat / Open / Stops wicking | Phys | Operation / Repeatable | Simple low-cost paper device. No moving parts. Simple electrical control (5V). Fast and repeatable. | To keep valve closed requires constant power (1.5A, 7.5W). Evaporation changes liquid concentration. High temperature (>60˚C) may damage the sample and alter reactions. |
| L. Cai, M. Zhong, H. Li, C. Xu and B. Yuan, *Biomicrofluidics*, 2015, **9**, 046503. | Printed surfactant, which solubility depends steeply on temperature, is used to assist the liquid to cross the hydrophobic barrier. Wicking rate depends almost linearly on temperature, complete closure at <15˚C. | Temperature / Either Open or Closed / Wicking speed modulation | Chem | Operation / One time | Simple low-cost paper device. No moving parts. Electrical control possible with heater/cooler. Adjustable flow rate. | Complete closure requires active cooling (15˚C). High temperature (80˚C) may affect chemistry or destroy sample. Surfactant may interfere with the assay. |
| A. W. Martinez, S. T. Phillips, Z. Nie, C.-M. Cheng, | Push-button 'on' valves, which are formed in multilayer paper device, where there is a cavity left between different paper | Mechanical pressing by user / Closed / Discrete opening | Phys | Operation / On time | Simple low-cost paper device. No chemical interference. | Mechanically moving parts. Automation would require more complex actuators |

| | | | | | | |
|---|---|---|---|---|---|---|
| E. Carrilho, B. J. Wiley and G. M. Whitesides, *Lab Chip*, 2010, **10**, 2499–504. | layers, which liquid cannot cross. Once pressed, cavity collapses and liquid connection between the paper layers is formed. | | | | | |
| S. Jahanshahi-Anbuhi, P. Chavan, C. Sicard, V. Leung, S. M. Z. Hossain, R. Pelton, J. D. Brennan and C. D. M. Filipe, *Lab Chip*, 2012, **12**, 5079–5085. | Flap valve, in which a paper cantilever is connecting or disconnecting the channel | Mechanical motion by user / Either Closed or Open / Discrete switching | Phys | Operation / Reversible | Fast switching, Reversible. No chemical interference. | Mechanically moving parts. |
| X. Y. Liu, C. M. Cheng, A. W. Martinez, K. A. Mirica, X. J. Li, S. T. Phillips, M. Mascareñas and G. M. Whitesides, in *IEEE MEMS*, 2011, pp. 75–78. | Sliding strip, which is moving between two stationary paper layers and can reconfigure the fluidic pathways between them. It allows to switch the sample between different liquid sources, operating as "selector switch". | Mechanical motion by user / Various states. Selector switch / Discrete switching | Phys | Operation / Reversible | Versatile to reconfigure the circuitry of flow paths. No chemical interference. | Mechanically moving parts. Automation would require more complex actuators. |
| X. Li, X. Li, J. Tian, J. Tian, T. Nguyen, T. Nguyen, W. Shen and W. Shen, *Lab Chip*, 2008, **80**, 9131–9134. | Simple sliding and cantilever valves, made by mechanical cutting assembly of hydrophilic/hydrophobic paper. | Mechanical motion by user / Either Closed or Open / Discrete switching | Phys | Operation / Reversible | Simple low-cost paper device. Reversible actuation. No chemical interference. | Mechanically moving parts. Automation would require more complex actuators. |
| B. J. Toley, J. A. Wang, M. Gupta, J. R. Buser, L. K. Lafleur, B. R. Lutz, E. Fu and P. Yager, *Lab Chip*, 2015, **15**, 1432–1444. | Liquid triggered expanding actuators (cellulose sponges) are used to mechanically move paper cantilevers and connect, disconnect or divert fluid flow paths. Actuation requires 30μL of fluid. | Liquid / Open or Closed / Discrete switching of flow path | Phys | Operation / One time | No chemical interference. Number of different functions. All regulation on chip. No external control required. Self-regulating liquid networks. | Mechanically moving parts. Complex device structure. Relatively slow (5-50s). No external control possible. |
| H. Chen, J. Cogswell, C. Anagnostopoulos and M. Faghri, *Lab Chip*, 2012, **12**, 2909. | Lateral flow fluidic diode, which uses deposited surfactant to cross the hydrophobic barrier. Liquid can initially pass only, when it arrives to the diode from surfactant side. Valve, once opened, conducts in both ways. | Liquid / Closed / Discrete opening | Chem | Operation / One time | Simple low-cost paper device. No moving parts. Self-regulating. No external control required. | Actuation program is set during manufacturing. Surfactant may interfere with assay. |

| | | | | | | |
|---|---|---|---|---|---|---|
| R. Gerbers, W. Foellscher, H. Chen, C. Anagnostopoulos and M. Faghri, *Lab Chip*, 2014, **14**, 4042–9. | Vertical flow fluidic diode (similar to previous). Two layers (one hydrophobic and another one containing dried surfactant) are stacked. Valve is opened, when liquid is wicking from the surfactant side, which allows it to pass the hydrophobic barrier. Valve, once opened, conducts in both ways. | Liquid / Closed / Discrete opening | Chem | Operation / One time | Simple low-cost paper device. No moving parts. Self-regulating. No external control required. | Actuation program is set during manufacturing. Surfactant may interfere with assay. |
| B. R. Lutz, P. Trinh, C. Ball, E. Fu and P. Yager, *Lab Chip*, 2011, **11**, 4274. | Valve based on the competing flows from a limited liquid source, which leads to the disconnection and delayed shut-off. | Liquid / Open / Discrete closure | Phys | Fabrication / One time | No external control required. No chemical interference. | Relatively complex setting to form competing wicking, which combines bulk liquid source and paper device. |
| **Passive flow-control methods for wicking-based paper microfluidic devices** | | | | | | |
| B. Lutz, T. Liang, E. Fu, S. Ramachandran, P. Kauffman and P. Yager, *Lab Chip*, 2013, **13**, 2840–7. | Dried sugar is used in the paper, which alters the liquid viscosity and wicking time | Liquid / N/A / Wicking speed modulation | Chem | Fabrication / One time | Simple low-cost paper device. No external control required. | Wicking properties are set during manufacturing (sugar deposition). Dissolved sugar may interfere with assay. |
| I. Jang and S. Song, *Lab Chip*, 2015, **15**, 3405–12. | Flow control based on wax printing method. Printing small amount of wax into the channels allows reducing the flow rate controllably. | Wax amount / N/A / Wicking speed modulation | Phys | Fabrication / N/A | Simple low-cost paper device. No moving parts. | Flow properties are set during manufacturing. |
| C.-H. Weng, M.-Y. Chen, C.-H. Shen and R.-J. Yang, *Biomicrofluidics*, 2014, **8**, 066502. | Wax printed valves. Thin wax print between the paper layers is liquid permeable, but once heated to 150˚C for 30min the wax wicks into the paper and makes it liquid impermeable (valve is closed) | Temperature / Open / Discrete closure | Phys | Before operation / N/A | Simple low-cost paper device. No moving parts. | Valve state has to be set by heating step before the operation. High temperature may damage reagents stored in the device. |
| J. H. Shin, J. Park, S. H. Kim and J. K. Park, *Biomicrofluidics*, 2014, **8**. | When porous mesh, like paper is mechanically treated by high-pressure press, material is compressed, which reduces the pore size, and increases the fluidic resistance, reducing the wicking speed. Wicking speed was reduced up to 740% by pressing (max 300bar) | Mechanical pressure / Open / Wicking speed modulation | Phys | Before operation / N/A | Simple low-cost paper device. No moving parts during operation. No chemical interference. Adjustable flow rate. | Requires high-pressure press to adjust the valve (300bar). Valve is normally set before operation. No complete closure possible. |
| D. L. Giokas, G. Z. Tsogas and A. G. Vlessidis, *Anal. Chem.*, 2014, **86**, | They use razor cuts in the paper channels to modulate the flow rates. Longitudinal channels increase the flow rate, while perpendicular ones decrease | Mechanical cut / N/A / Wicking speed modulation | Phys | Fabrication / N/A | Simple low-cost device. No moving parts. Extends the range of flow rates possible. No chemical interference. | Flow properties are set during the manufacturing. |

| | | | | | | |
|---|---|---|---|---|---|---|
| 6202–6207. | | | | | | |
| B. J. Toley, B. McKenzie, T. Liang, J. R. Buser, P. Yager and E. Fu, *Anal. Chem.*, 2013, **85**, 11545–52. | Absorber pads (shunts) are placed on the lateral-flow paper channel in order to delay the wicking front. It gives a fixed delay, after which the wicking continues at the same rate. Though not shown, it can be imagined that shunt is actively connected/disconnected also during the operation. | N/A / N/A / Wicking delay | Phys | Fabrication / N/A | Simple low-cost device. No moving parts. Delays wicking, but does not slow down the later flow, as longer channel would do. No chemical interference. Adjustable delay time by shunt geometry. | Extra sample required for filling the shunt. Pre-defined delay. No external control. |
| S. Jahanshahi-Anbuhi, A. Henry, V. Leung, C. Sicard, K. Pennings, R. Pelton, J. D. Brennan and C. D. M. Filipe, *Lab Chip*, 2013, **14**, 229–236. | Water-soluble Pullulan films, have been placed over small gap in the paper channel. Initially liquid passes the gap, but when Pullulan dissolves, liquid becomes substantially more viscose and flow slowes/stops. This provides delayed shut-off of the flow. | Liquid / Open / Wicking speed modulation | Chem | Fabrication / One time | Simple low-cost device. No moving parts. No external control required, Adjustable flow rate and shut-off by the film geometry | Actuation program is set during manufacturing. Dissolved polymer may interfere with the assay. Actuation may depend on parameters such as room temperature. No complete closure. |
| **Other paper microfluidic devices with flow control** | | | | | | |
| H. Ko, J. Lee, Y. Kim, B. Lee, C.-H. Jung, J.-H. Choi, O.-S. Kwon and K. Shin, *Adv. Mater.*, 2014, **26**, 2335–40. | Traditional type of electro-wetting to move droplet, on the surface, but the device substrate is paper. Electrodes are printed with carbon ink and coated with parylene and fluorocarbon oil. | Electrical signal / N/A / Droplet motion | Phys | Operation / Reversible | Printed. Fast actuation. Flexible substrate. | Relatively complex fabrication. Not compatible with wicking-based paper microfluidics. |
| **Flow control technologies, which could be relevant for paper microfluidic applications** | | | | | | |
| G. Londe, A. Chunder, A. Wesser, L. Zhai and H. J. Cho, *Sensors Actuators, B Chem.*, 2008, **132**, 431–438. | PNIPAAm and silica nanoparticles based surface treatment, which hydrophobic/hydrophilic state is switched by temperature. Above 65˚C it is hydrophobic and below that hydrophilic. This device is shown in glass microfluidics, but principle would be compatible with paper devices as well. | Temperature / Closed / Discrete opening | Phys | Operation / One time | No moving parts. Simple electrical control by heating. | More complex fabrication. High temperature may damage sample or reagent and require higher heating power. |
| M. Xiong, B. Gu, J. D. Zhang, J. J. Xu, H. Y. Chen and H. Zhong, *Biosens. Bioelectron.*, 2013, **50**, 229–234. | Photopatterned PNIPAAm film is used to modulate surface wettability and reversibly release and adsorb GOx to switch on and off the enzymatic reaction. | Temperature / N/A / Chemical switch | Chem | Operation / Reversible | Simple low-cost device. No moving parts. External control can be achieved by heating and cooling. Actuation temperature is mild. | Temperature may affect other aspects of chemistry. Since actuation temperature is about 35˚C, switching may require active cooling. |
| G. Chen, F. Svec and D. R. Knapp, | PNIPAAm based microvalve, which is actuated by high power | Light induced temperature change / | Phys | Operation / Reversible | No moving parts. Simple electrical control by light. | High temperature may damage sample or reagent |

| | | | | | | |
|---|---|---|---|---|---|---|
| *Lab Chip*, 2008, **8**, 1198–204. | light, that causes heating. Valve opens and closes in few seconds | Closed / Discrete opening | | | Reversible actuation. | and require higher heating power (light source). |
| T. Guo, T. Meng, W. Li, J. Qin, Z. Tong, Q. Zhang and X. Li, *Nanotechnology*, 2014, **25**, 125301. | Microchannel coated with a layer of silanized $TiO_2$-$SiO_2$ nanoparticles. This layer is normally hydrophobic and repels the liquid, but becomes hydrophilic when exposed to UV light, which degrades the organic layer from its surface. Hydrophobicity recovers in 2weeks. This is not paper device, but idea could be compatible. | UV light / Closed / Wicking speed modulation | Chem | Before operation / Reversible (but slow) | Simple low-cost device. No moving parts. | Long switching time and high doze of UV (12W, 254nm for 6h). Shown only as pre-operation modification. |
| F. He, J. Grimes, S. D. Alcaine and S. R. Nugen, *Analyst*, 2014, **139**, 3002–8. | They use silver electrode, which has surface assembled monolayer of hydrophobic fluorinated thiol. Liquid normally does not cross the electrode, until voltage in the range of 2-4V is applied, which erodes the coating and wets the electrode. This is not a paper device, but elastic channel made in PET film. | Electrical signal / Closed / Discrete opening | Chem | Operation / One time | Simple low-cost device. No moving parts. Simple low-voltage electrical control. | Electrochemical reaction may damage sample/reagents. Relatively slow (10-40s). |
| B. Mosadegh, A. D. Mazzeo, R. F. Shepherd, S. a Morin, U. Gupta, I. Z. Sani, D. Lai, S. Takayama and G. M. Whitesides, *Lab Chip*, 2014, **14**, 189–99. | Braille display is used to actuate elastomeric valves. Same principle could be also used to actuate paper valves based on cantilevers and push-button. This would allow automation of assays. | Electro-mechanical actuator / N/A / N/A | Phys | Operation / Reversible | Allows automation of paper devices with mechanical valves. Many channels. Can be reversible. No chemical interference. | Braille display is a more expensive component. |
| G. Korir and M. Prakash, *PLoS One*, 2015, **10**, 1–17. | Punch card and sound box can be used to actuate elastomer based microfluidic valves, but same principle could be also used to actuate paper valves based on cantilevers and push-button. This would allow automation of assays. | Multi-channel mechanical actuation program / N/A / N/A | Phys | Operation / Reversible | Allows automation of paper devices with mechanical valves. Many channels. Can be reversible. Low-cost and simple. No chemical interference. | No electronic control |

**Preparation of conductive paper for electrowetting**

Electronically conductive paper was prepared by coating Whatman lens paper 105 with carbon ink. We prepared the carbon ink by dissolving carboxymethyl cellulose sodium salt (CMC, average M.W. 250'000g/mol, DS=1.2, obtained from Acros Organics) in de-ionized water (DIW) with a concentration of 10mg/mL. We added 300mg of multiwall carbon nanotubes (MWCNT, average outer diameter 6-9nm and length 5µm, obtained from Sigma-Aldrich, product code: 724769), to 10mL of the CMC solution and 20mL of DIW and dispersed the mixture for 15 min. using a Branson high-power sonifier 340, at a duty cycle of 50% and output power of 400W. The resulting ink was further diluted 50% in DIW. The lens paper was soaked into the ink solution; we used tissue papers to remove the excess ink and dried the lens paper in air. Subsequently, we hot pressed the lens paper at 210˚C for 1 min. to improve flatness. The properties of conductive paper for electrowetting are listed in table S2.

**Table S2.** Properties electrically conductive paper as a material for electrowetting.

| **Property** | **Paper** |
|---|---|
| Initial Substrate | Whatman Lens paper 105 |
| Conductive coating | Dip-coating with multi-wall carbon nanotube ink |
| Insulation layer | ~10µm Parylene-C |
| Hydrophobic layer | Dip-coating with 0.2% solution of Teflon AF 2400 |
| Resistivity (Ohm/sq.) | 7700 |
| Fiber diameter (µm) | ~20 |
| Opening size (µm) | ~10 (large distribution) |
| Period (µm) | Non periodic |
| Thickness (µm) | 45-50 |
| Liquid breakthrough pressure (mbar) | 12.6 ($\sigma = 3.8$) |
| Substrate cost (USD/cm$^2$) | 0.00023 |

**Parylene-C and Teflon coating of textiles and paper**

The coating procedure was as follows: i) Samples were cleaned with a mixture of IPA:water (1:1) and primed with adhesion promoter Silquest A-17-NT silane (Chempoint, Bellevue, WA). ii) Samples were loaded in a deposition chamber, which was pumped overnight followed by coating at rate about 5μm/h. During coating samples were rotated in the chamber to improve thickness uniformity. Although the dimer precursor of parylene is pyrolized at high temperatures (680˚C) samples are not heated and stay at RT throughout the process. Thickness was estimated from deposition time and no online feedback was used. After completion, the thickness was measured on a sample piece and was found to be 11μm (target was 10μm). Parylene coating would be compatible with low-cost manufacturing. Due to large chambers one run (250USD) would allow production of material sufficient for a large number of devices.

Teflon AF 2400 (powder) and fully fluorinated solvent 3M Fluorinert® FC-40 were purchased from Sigma-Aldrich. A solution was prepared in a small glass jar, with Teflon® AF (w/w 1%). The jar was placed in a 50˚C water bath, and the mixture was stirred with magnetic stirrer for about 24h until complete dissolution. The 1% stock solution was further diluted into 0.2% solutions in the same solvent, and the textiles were dip-coated in this solution. The coated samples were dried first at ambient atmosphere for a minimum 15min, followed by 3h baking in an oven at 130˚C. Coatings of Si wafers (for contact angle measurement) was done using spin-coating at 4000rpm for 1min followed by same baking procedure.

**Measurement of liquid breakthrough pressure for different textiles**

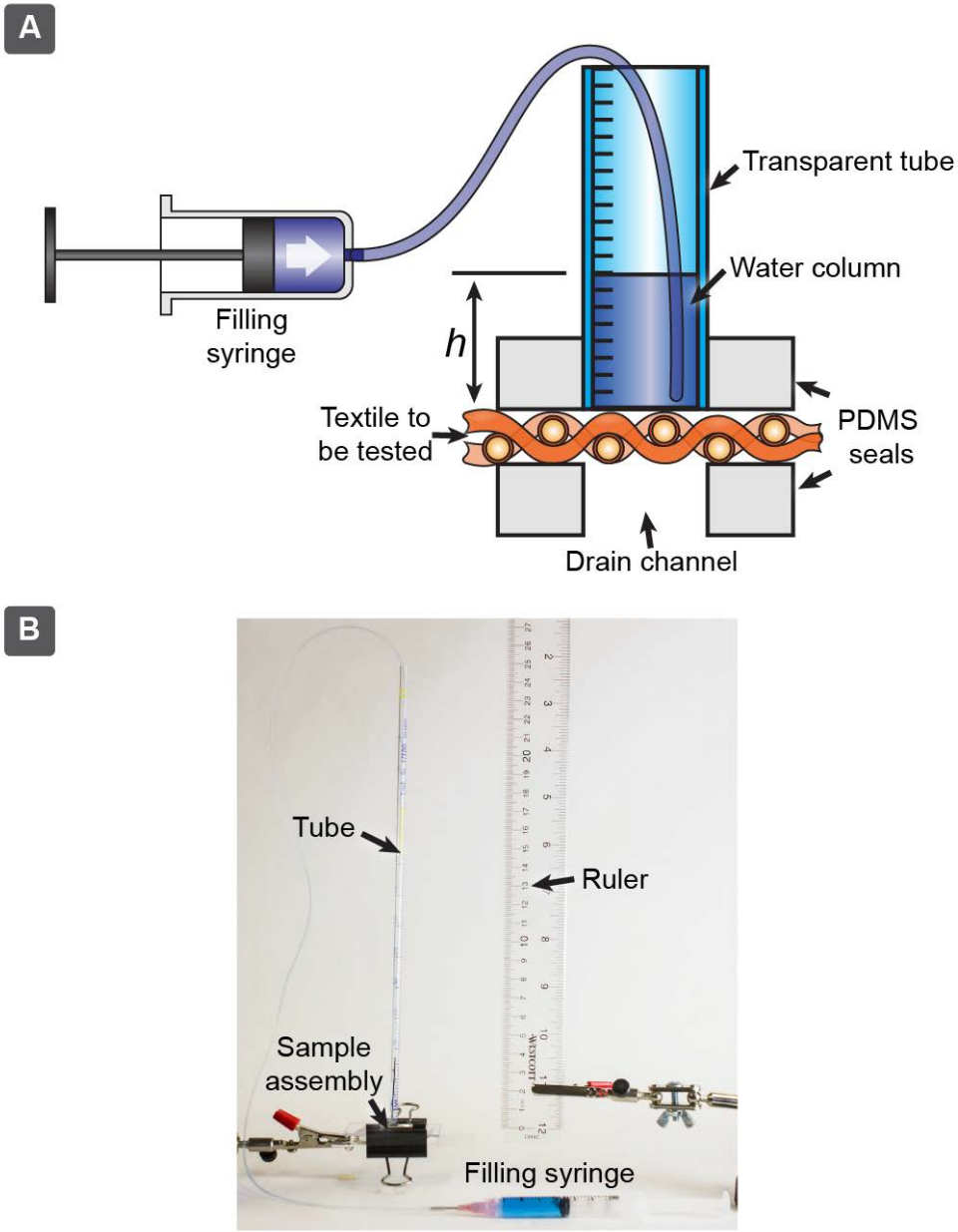


**Figure S1.** (A) Schematic diagram of a liquid breakthrough pressure measurement setup and (B) photo of it. As a transparent tube we used 10mL polystyrene serological pipette (I.D. 2.7mm). Measurement was carried out as liquid breakthrough into open drain channel.

**Theory and basic characterization of electrowetting through textiles**

To roughly describe this complex process with a simple model, we can consider the pressure $p$ required for the liquid to pass through a porous material as given by the Washburn equation (Equation S1)

$$p = -\frac{4\sigma cos\theta}{d_p} \tag{S1}$$

here $\sigma$ is surface tension of the liquid, θ is the advancing contact angle of the liquid on the surface of the porous material, and $d_p$ is an average or effective diameter of the pore. Since the textile is hydrophobic ( $\theta_0 = 105^\circ$), the pressure required to push a liquid through the textile is positive.

The contact angle θ can be modified via electrowetting (analogous to that of EWOD) by application of a voltage $U$ according to the Lippmann-Young equation (Equation S2)

$$cos\theta = cos\theta_0 + \frac{\varepsilon\varepsilon_0 U^2}{2\sigma d_i} \tag{S2}$$

$\theta_0$ is the initial Young's contact angle, $\varepsilon$ is the dielectric permeability of the layer of insulation on the wires (3.15 for Parylene-C), and $d_i$ is the thickness of the insulation layer (~10μm Parylene-C). Combining equation S1 and equation S2, we can see that an activation voltage $U_a$ is required to trigger liquid flow through the textile (this happens when $p \approx 0$), according to (Equation S3).

$$U_a = \sqrt{-\frac{2\sigma d_i cos\theta_0}{\varepsilon\varepsilon_0}} \tag{S3}$$

To measure contact angles as a function of liquid surface tension, we used mixtures of ethanol (EtOH) and water to vary the surface tension in the range from 22mN/m (pure ethanol) to 72 mN/m (water), and measured the contact angle of the different mixtures as a function of applied voltage (Figures S3 A) on a Si-wafer coated with Parylene-C (11 μm) and Teflon AF. This data correlated well with equation 2 up to around 200 Volts (the Lippmann-

Young regime), but the contact angle did not change much as a function of voltage above 200V (this is known as the saturation regime). The deviation from theory in the saturation regime is not yet explained with a unified theory.

Next, we measured the actuation voltage for the different solutions on an aluminum textile coated with Parylene-C (11 μm), and Teflon AF (Figure S2). We could not determine an actuation voltage in case of 100% EtOH, since this solution penetrated through the textile without an applied potential. The highest EtOH concentration measured was 50%. Figure S4B shows the measured data vs. the theoretical value calculated from equation S3, using the material parameters $\frac{2\sigma_i d}{\varepsilon\varepsilon_0}$ where $d = 11\mu m$, $\varepsilon = 3.15$,

$\sigma_i = 72\frac{mN}{m}(water),\ 56\frac{mN}{m}(5\%\ EtOH),\ 48\frac{mN}{m}(10\%\ EtOH),\ 29\ \frac{mN}{m}\ (50\%\ EtOH)$, and

$\theta_0$ is the initial Young's contact angle from the experimental measurements on planar surfaces.

We observed relatively large device-to-device variability in the minimal voltage threshold required to open a valve ("actuation voltage"), this is most likely due to the three dimensional nature of woven mesh combined with local variability in the thickness of coatings compare to, for example, planar EWOD devices. We also noticed that during the actuation the flow through the gate mesh starts at certain point or few points rather than through entire mesh instantaneously.

To summarize, we showed that the valves could function even for a liquid with an initial contact angle of $\theta_0$=83˚ (surface tension 28mN/m). We derived a simple theoretical model (Equation S3) to calculate the threshold voltage of the valve actuation, and showed that this model works for estimating the actuation voltage but does not fully describe this system.

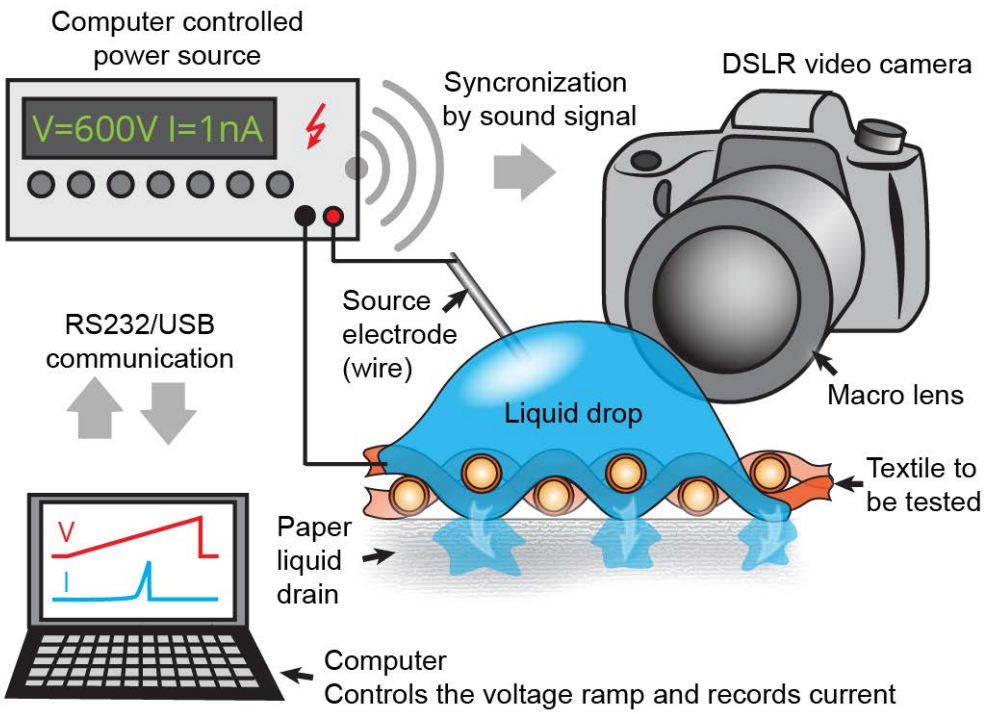


**Figure S2**. Experimental setup used to determine the actuation voltage of textile valves.

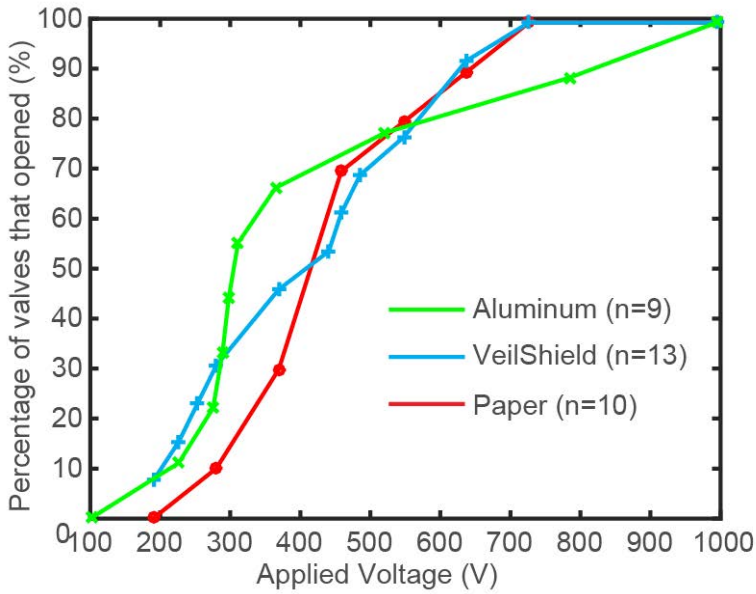


**Figure S3**. Percentage of valves (devices), which opened at certain voltage threshold, during the voltage ramp from 0 to 1000V. We tested the voltage response for three different materials: Aluminum, a plastic woven mesh with a conductive coating (see Table 1), and paper coated with a conductive carbon nanotube layer (see Table S2). Each material was tested for n different devices.

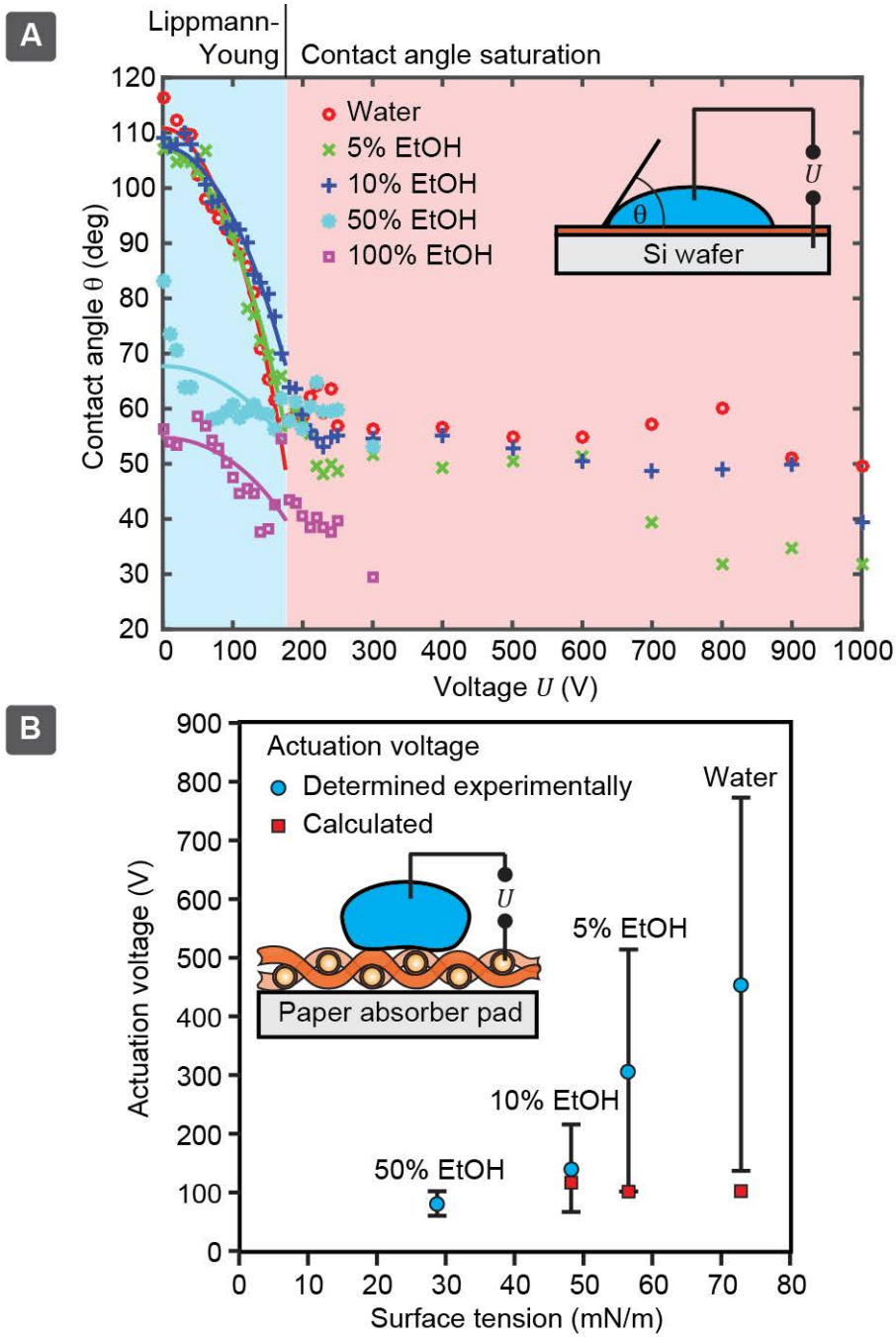


**Figure S4**. (A) Contact angle measurements of different EtOH solutions in water measured on Si-wafer with Parylene-C (10µm) and Teflon AF coatings. Contact angles at low-voltages (Lippmann-Young regime) were fitted to Lippmann-Young equation. (B) Actuation voltage of an aluminum textile with Parylene-C (10µm), and a thin Teflon AF coating, measured as a function of liquids with different surface tension, (water with different ethanol content). The theoretical values are calculated using equation S3.

**Influence of ionic strength on the actuation voltage**

We studied the dependence on ionic strength on the actuation voltage by using the same method and setup as described earlier. Here we used 20 µL droplets of 1 µM, 1 mM and 1 M KCl solutions to test the dependence of ionic strength on actuation. We could not observe any notable difference on DC actuation voltage in this concentration range as shown on Figure S5. This result is expected based on previous findings [Quinn et al. J. Phys. Chem. B 2003, 107, 1163-1169]. In these systems, the conductivity is expected mainly to affect the AC electrowetting [Kumar et al, Mater. Res. Soc. Symp. Proc. Vol 899, 2006]. We also did not observe any significant difference on the electrical current during valve actuation or the liquid flow rate through the valves.

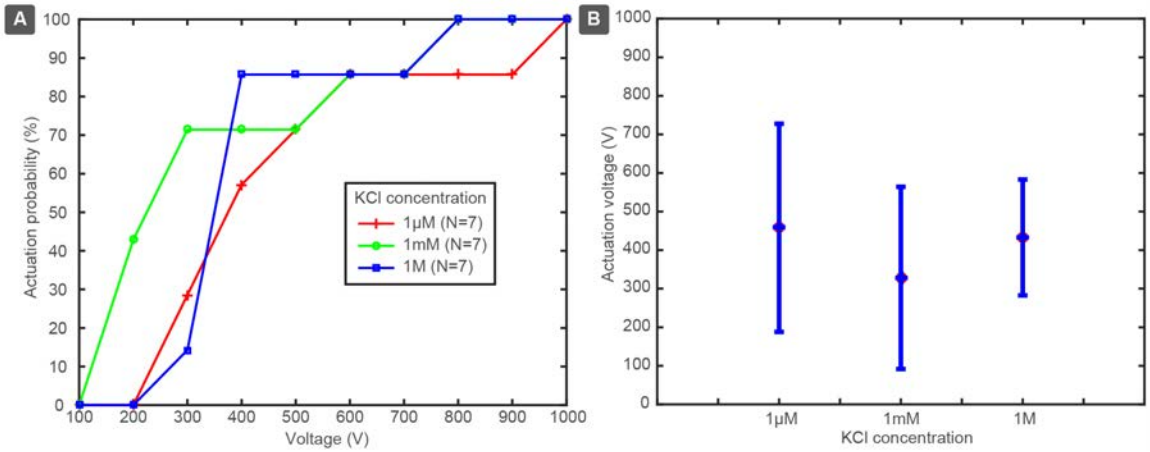


**Figure S5.** (A) The percentage of valves, which opened at certain voltage threshold during the voltage ramp from 0 to 1000V (N=7 devices). We measured the voltage responses for three solutions of varying ionic strength. (B) The average actuation voltage with standard deviation for the same experiment

**Effect of the pulse length on valve actuation**

To test the effect of pulse length on actuation, we used pulsed actuation voltage instead of a slowly ramped DC voltage. The electronic part of the setup was fabricated as shown on Figure S6A. We supplied an input voltage of 500 V and pulse-modulated the voltage using an N-CH MOSFET transistor FQN1N50CTACT (500 V, 380 mA). The gate of the transistor was controlled using a 80 MHZ arbitrary waveform generator Agilent 33250A, with digital signal output (levels 0 and 6 V). We varied the pulse length and number of pulses delivered. The Pulsing was triggered manually. We then monitored the flow rate of a coloured solution (Orange G in milli-Q water) into 5 mm diameter paper area with a camera Canon EOS (50 fps), and used a MATLAB based image analysis software to determine the filling time of the paper area as a measure of the valve opening. The filling was roughly proportional to the time after opening as seen on figure S6B. As a characteristic time-constant, we used the time required to fill the paper pad from 20 to 80%. In the first test we monitored 10 valves, while increasing the length of single voltage pulses in steps of 100 μs, 1 ms, 10 ms, 100 ms, 1 s. The 100 μs pulse was not able to trigger the valve, while the 1 s pulse triggered all valves (Figure S6C). Using shorter pulses yielded variable filling times (Figure S6D). There was, however, no clear correlation between the pulse length and the filling rate. Longer (1 s) pulses caused faster rate of filling. In a second test, we used 1 ms “on” 1 ms “off” pulses, but varied the number of pulses (5, 10, 20 pulses). Using sequence of 20 pulses yielded faster flow rate in all tests, with overall shorter control signal (total length of pulse sequence 40 ms). This result suggests that using pulsation could be efficient way to improve speed of opening of the valve, but using variable pulse length does not seem to be sufficiently reproducible to be exploited as a mean of control of flow rate.

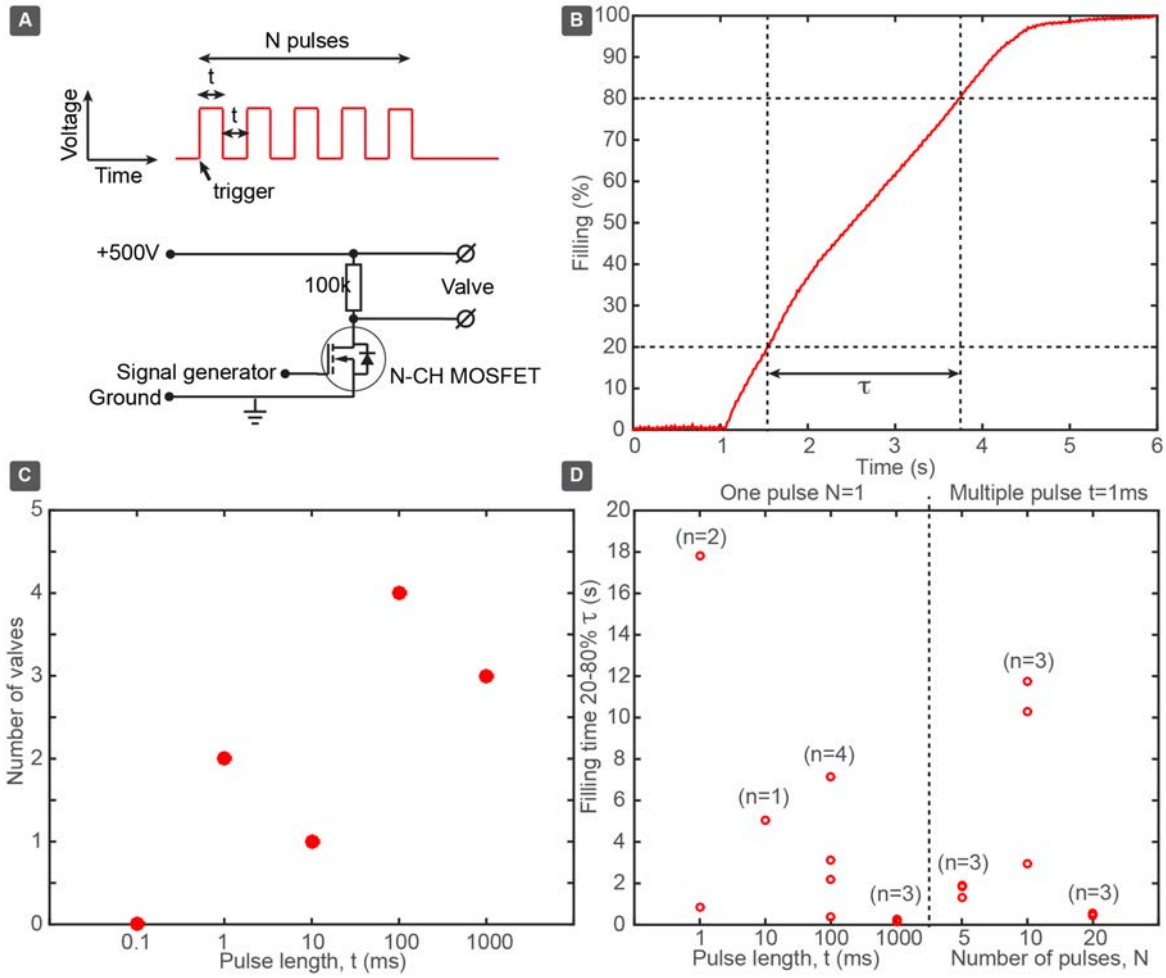


**Figure S6.** (A) The circuit diagram for pulse modulation device. (B) Filling of a 5-mm diameter paper pad, that is filled with a solution through a valve. (C) Minimal 500 V pulse length required to open the valve (n=10 devices). (D) Comparison of filling time depending on pulse length and number of pulses.

**Textile valves as "electrofluidic thyristors"**

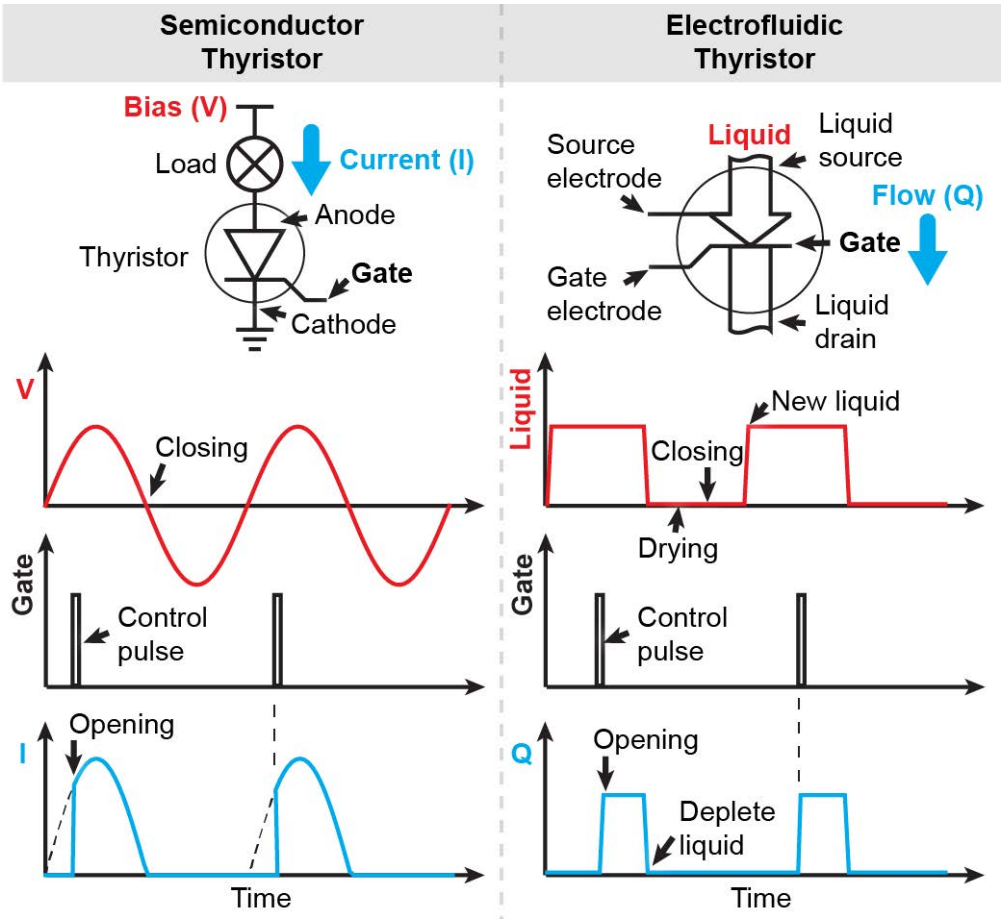


**Figure S7.** Schematic circuit diagrams and electrical function of a semiconductor thyrisor (left) vs. a fluidic thyrisor (right). Experimental repeated bistable actuation is demonstrated on following figure S8.

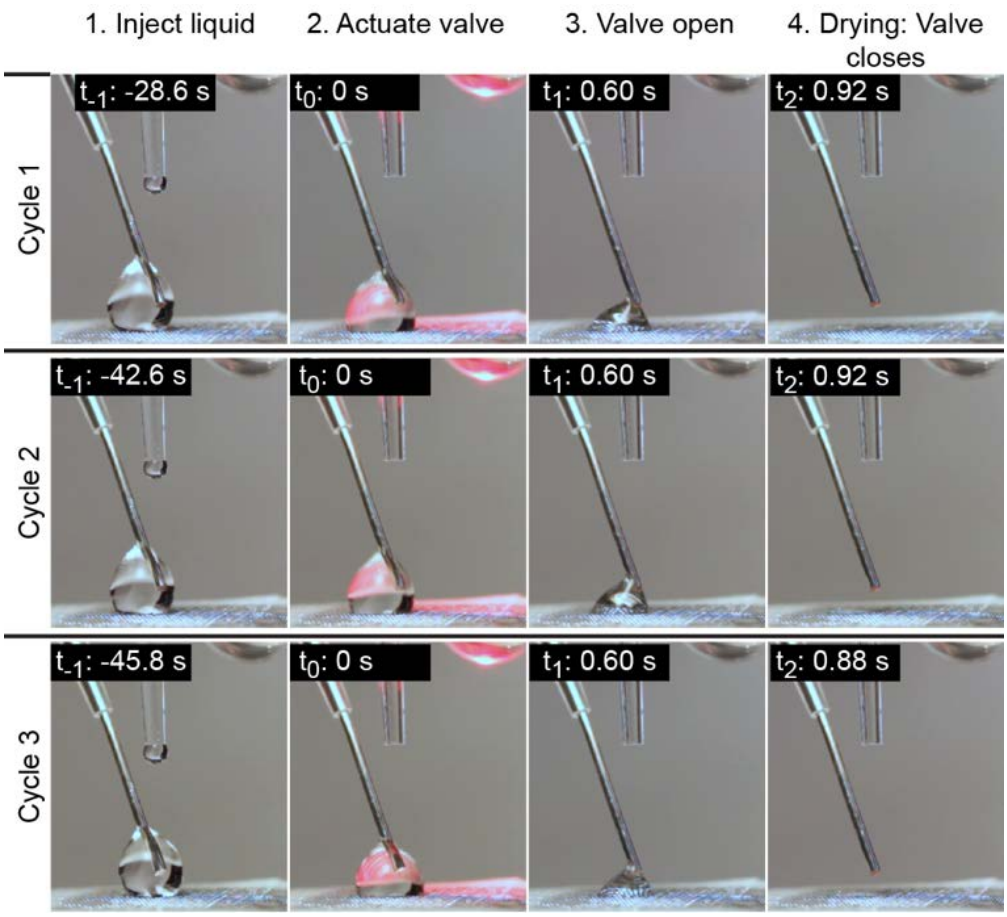


**Figure S8**. Time-lapse photos showing the function of a bistable electronically actuated liquid valve with three consecutive actuation cycles. Each cycle consists of: i) application of liquid (water), ii) opening of the valve with an electrical pulse, iii) liquid flow until the droplet has been depleted, and iv) drying of valve (restoration to the initial state).

**Angle dependence**

We tested valve actuation, when device is at different angles relative to the Earth ground. Since the angle cannot be changed in open textile configuration, as droplets would slide or drop off from the bare hydrophobic surface, we have embadded the textile (Aluminum) between two paper layers. Both paper layers had printed wax barriers surrounding circular hydrophic area (liquid source and drain. Source side is green and drain side is blue. Hydrophilic area had printed diameter 7.5mm). For electrical conductivity, source side had painted conductive ink electrode. Gate textile was directly connected with aligator clip. As a

liquid we used water, which was stained with acid red in order to facilitate visualization. Each time we loaded 20µL of liquid. We varied the angle from 0˚ (horizontal, droplet on top of paper) to 180˚ (upside down, droplet was hanging on the hydrophilic paper). All actuation voltages (Figure S9 A) were in the same range as measured at horizontal position (Figure S3B water), which is expected as capillary force is dominating over the gravity in case of small droplet (pressure from liquid column height is much lower than liquid breakthrough pressure)

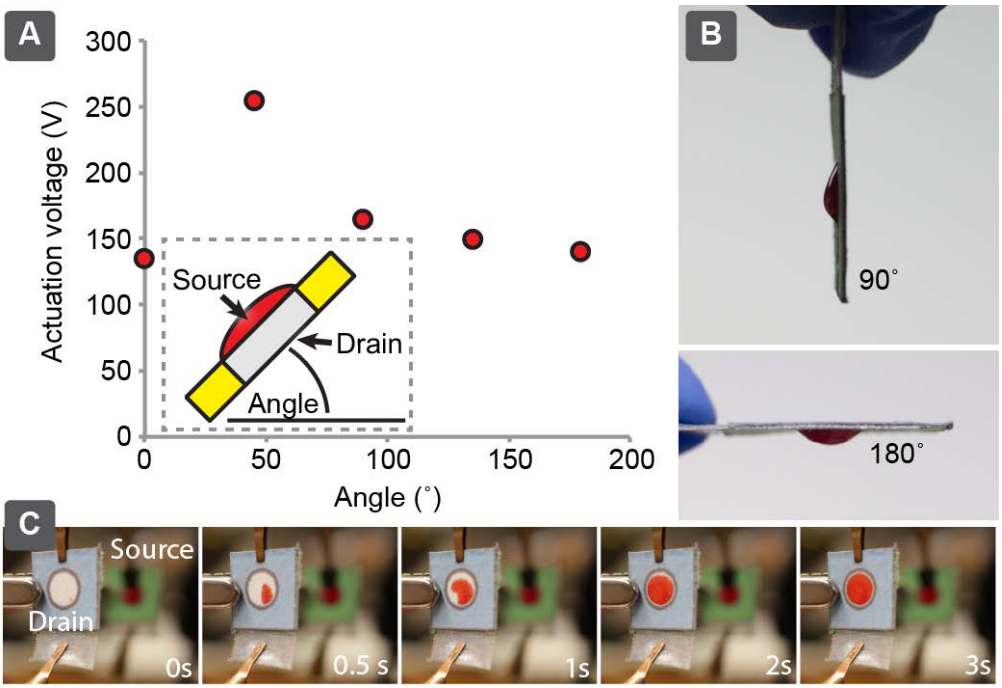


**Figure S9**. A) Measured actuation voltage depending on the angle. B) Liquid drop on the device source as seen at different angles. C) Exemplary time series of valve actuation at 90˚.

## Logic control

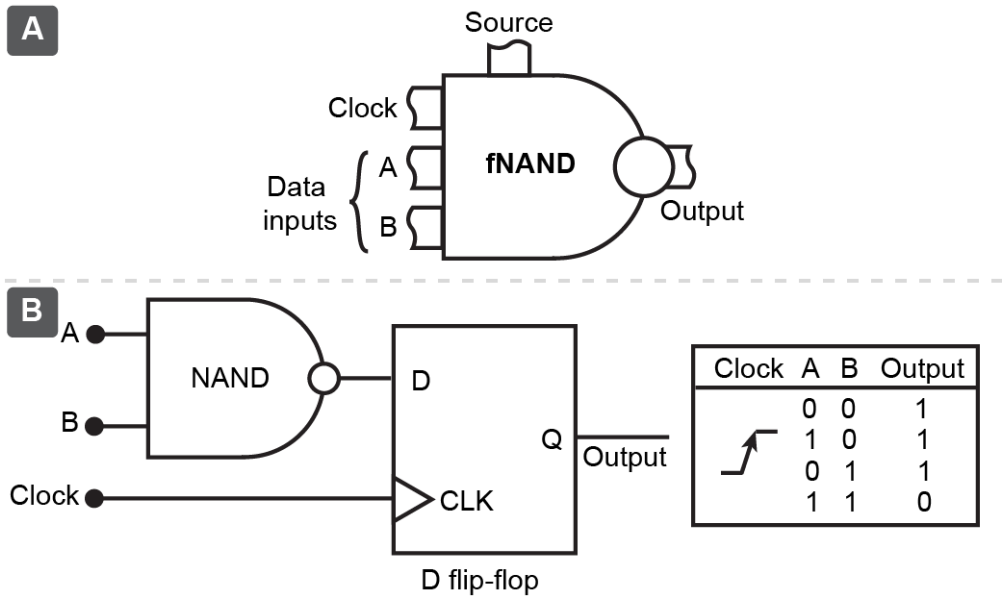


**Figure S10**. Fluidic NAND gate (fNAND) (A) Proposed symbol for fluidic fNAND. (B) Corresponding electronic equivalent scheme, which contains NAND gate and D flip-flop, and where the output of the NAND gate is coupled through the flip-flop.

## Low-cost high-voltage power supply

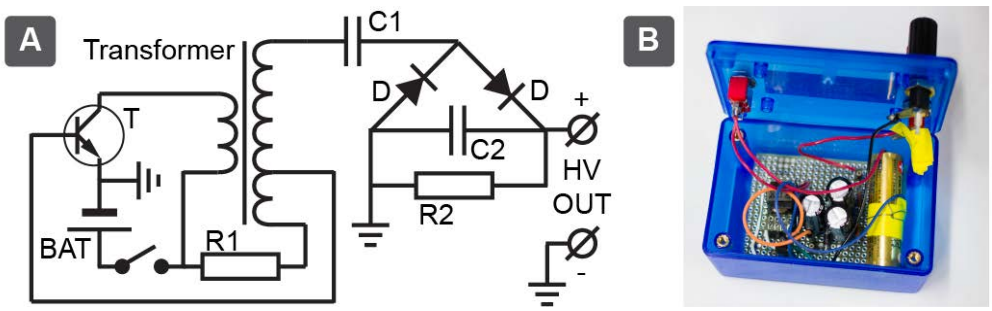


**Figure S11.** *High voltage at low-cost*. (A) Circuit diagram of a low-cost single-channel high voltage power supply sufficient to actuate the valves. We obtained all essential components of the power supply from the flash mechanism of Fujifilm disposable camera purchased from Amazon for 9.5USD. This circuitry was powered by a single AA battery (1.5V). Power supply contained following components: transformer (coil inductances 49µH, 100µH and 2H),

NPN transistor (D2504), two diodes (1N4007), capacitors (C1, C2: 10μF), and resistors (R1: 220Ohm, R2: 2MOhm). These were arranged functionally into a two-part oscillator with high-voltage transformer (Output: Vrms: 390V, 13kHz) and diode ladder/rectifier. The power supply had maximum output voltage of 650V and maximum current 3mA. The output voltage dropped linearly with current, giving internal resistance about 217kOhm. (B) Photo of the high voltage device. We measured the power consumption of the power supply. Approximately constant current 80mA was drawn from a single AA battery (1.5V). In an about 5s the output voltage reached 650V (Total energy from battery: 0.6J). At 100mA current load regular AA batteries (e.g. Energizer E91) have been specified to provide 2500mAh charge, which would correspond to 22320 charging (actuation) cycles.

**Alternative high-voltage power supply design**

We constructed another high voltage (HV) control unit (Figure S12) in order to automatically actuate multiple valves with high time resolution as well as to demonstrate a another feasible design approach for low-cost portable instrumentation. The key components of this design are a miniature HV converter (rendering 5V to 3kV) and high voltage transistors, enabling on-off switching of individual channels at voltages up to 4.5kV (This was the highest voltage rating commercially available, low-cost and miniature transistor we found). The purchased price of the HV converter and transistors was 138 USD and 15.3 USD/each, respectively. Thus the cost of the key components was about 170 USD. Remaining components were much cheaper or have low-cost alternatives (e.g. Arduino board (~45 USD) can be replaced with low-cost microcontroller with price less than a dollar). Price of HV components drops rapidly with voltage (e.g. for 1kV the material cost would be <100 USD and for 200V it would be <50 USD). This unit was based on microcontroller board Arduino Due, which was programmed in

C and powered and controlled through computer USB port. The computer side software was created in Visual Studio .NET C++.

The device was characterized and had following features:

- Two high voltage digital outputs able to switch between 0 and set HV level
- Capability to deliver HV pulses with 1ms time resolution (but accuracy is significantly higher).
- Manually or automatically adjustable HV level between 300V to 2.7kV (no load).
- Maximum output current 33μA (short circuit).
- For instrument safety, full galvanic isolation between low (LV) and high voltage electronics (HV converter is isolated internally and control signals were coupled from LV to HV side through optocoupler. HV side control was powered with individual small battery).
- Computer communication through USB emulated serial port.
- Synchronization output to trigger any other instrument (e.g. camera) or LED, which can be incorporated into visual field in case of video recording of valve operation and enables easier analysis of response

**Materials.** HV converter was purchased from EMCO High Voltage Corporation (Sutter Creek, CA). High voltage transistors were purchased from Mouser Electronics (Mansfield, TX). All other standard electronic components were obtained from Mouser Electronics, Digi-Key Corporation (Thief River Falls, MN) or were provided by Electronic Instrument Design Lab in Harvard University, Department of Physics. The detailed listing of components is brought in Table S3

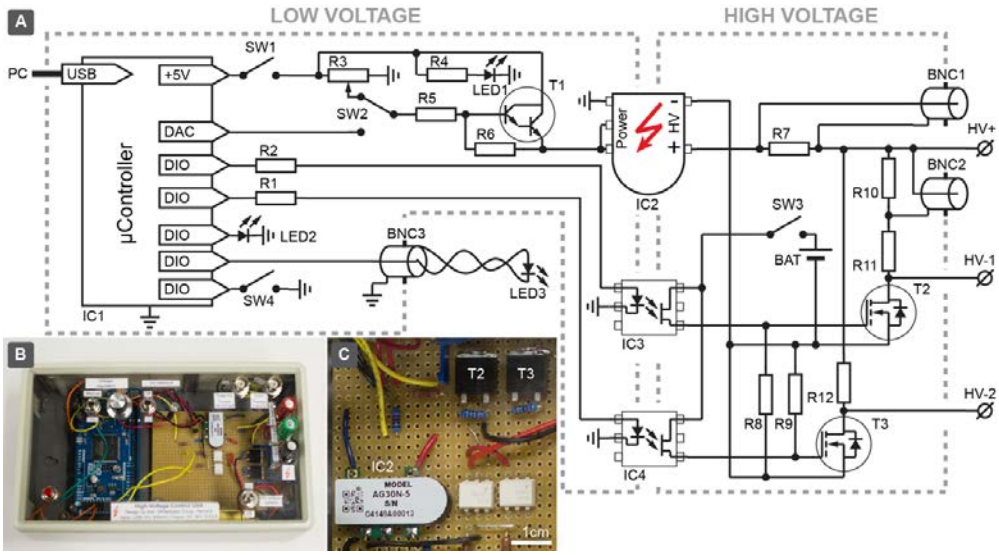


**Figure S12.** In-house built high voltage control unit. (A) Circuit diagram. (B) Photographs of a prototype device. (C) Photograph of the main parts of miniature high voltage electronics, showing 3kV high voltage converter (IC2) and 4.5kV FET transistors (T2 and T3). It shows that essential electronics could easily fit into a few cm sized portable module.

**Table S3.** List of components, for the high voltage device.

| Component | Type/Value | Description |
|---|---|---|
| **IC1** | Arduino Due | Microcontroller board based on Atmel SAM3X8E ARM Cortex-M3 CPU (32-bit ARM core microcontroller). But can be also substituted with much lower cost controller. |
| **IC2** | EMCO AG30N-5 | Miniature low to high voltage (HV) DC/DC converter (from 5V to 3kV). Input voltage 0.25-5V and current 200-470mA. Output voltage proportional to input in the range from 300V to 3kV with maximum output current 0.33mA and power 1W. Input and output side are galvanically isolated. |
| **IC3, IC4** | H11F1M | MOSFET optocoupler. Isolation voltage >5kV. |
| **T1** | 2N6426 | NPN Darlington transistor. Maximum current: 1.2A |

| | | |
|---|---|---|
| | | and amplification 20’000. For regulation of input voltage of HV converter. |
| **T2, T3** | IXTA02N450HV | n-channel MOSFET transistor. Maximum switchable voltage and current 4.5kV and 200mA. Gating threshold voltage: 4 to 6.5V Switching time <150ns. |
| **SW1** | Toggle switch | Powers HV circuitry. Safety interlock |
| **SW2** | Toggle switch | Switches voltage adjustment between manual and microcontroller regime |
| **SW3** | Toggle switch | Powers HV switching circuitry |
| **SW4** | Push button | For manual activation of output channel 1 |
| **HV+** | Plug connector | HV output common terminal (+) |
| **HV-1** | Plug connector | HV output channel 1 terminal (-) |
| **HV-2** | Plug connector | HV output channel 2 terminal (-) |
| **BNC1** | BNC jack | Total HV current monitor 10mV/μA |
| **BNC2** | BNC jack | HV output channel 1 voltage monitor 1V/kV |
| **BNC3** | BNC jack | Synchronization output. For external electronics or LED |
| **LED1** | LED | HV power indicator. If “on”, HV converter is powered |
| **LED2** | LED | Microcontroller status indicator |
| **LED3** | LED | Synchronization LED (for video recording) |
| **R1, R2** | 100 Ω | Optocoupler input LED current limiter |
| **R3** | 1 kΩ | Adjustable potentiometer for manual voltage regulation |
| **R4** | 1 kΩ | HV power LED current limiter |
| **R5** | 1 kΩ | T1 transistor base current limiter |
| **R6** | 10 kΩ | T1 transistor base pull down resistor |
| **R7** | 10 kΩ | Current monitor resistor |
| **R8, R9** | 10 kΩ | HV MOSFET pull down resistor |
| **R10** | 1 MΩ | HV output channel 1 voltage monitor resistor |
| **R11, R12** | 1 GΩ | HV output channel pull up resistor |

| | | |
|---|---|---|
| **BAT** | PP3 | 9V battery for powering the HV switching circuitry for full galvanic isolation. Could be substituted with low-cost DC/DC converter. |

**Iodate Assay**

Circular indicator pads (7mm diameter) were created using wax printing, as described before. 10 µL starch indicator was deposited on the pad and dried. First, we evaluated assay performance, by mixing the components in a test tube: 4µL of 1M p-toluenosulfonic acid, 2 µL of 0.5 M KI, 40 µL $KIO_3$ and 30 mM $Na_2S_2O_3$ solutions. We varied the $KIO_3$ concentration in series of 0, 0.1, 0.2, 0.5, 0.75, 1, 2, 3 and 5 mM and varied the volume of $Na_2S_2O_3$ in series 2, 4, 8 and 16 µL. After mixing, 10 µL of reaction product was transferred to the indicator pad. Visual change was recorded with a camera (Canon EOS 550D, EF-S 24 mm, and F2.8 lens). Colorimetric signal was evaluated using MATLAB, defined as a relative change in brightness (linear sum of individual RGB channels) of the indicator area. We then evaluated the storage of reagents in paper. Due to incompatibility, the input pad (circular 7mm diameter area) was divided into three equal sectors using 2pt line in Illustrator (a narrower line could not stop wicking). Same volumes of reagents were stored in these three sectors and dried in an oven at 60 ˚C until water had evaporated. First, we tested the assay without the valve by depositing 40µL of sample to the input pad, this amount of liquid was sufficient to cover the entire input pad and connect the individual sectors. Also since paper could not absorb the entire volume in its pores, an open drop left outside of the paper matrix would support convective mixing upon mechanical agitation. We used a custom built mechanical shaker shown in Figure S15. After 3 min of shaking, the reagent mixture was transferred to an indicator pad.

**Table S4.** Reaction can be limited by different components. If we denote the initial mole amounts of $K^+IO_3^-$, $I^-$, $I_3^-$, $S_2O_3^{2-}$ with *a, b, c, d* and end amounts with *A, B, C, D* respectively, we can calculate the end amounts of all reaction products or leftovers using the following equation systems. The amounts in the solution at the end must be equal to or larger than zero. Using the equations below, we can calculate the amounts at the end, for each initial combination.

| | **$K^+IO_3^-$ limited, $I^-$ in excess** | **$K^+IO_3^-$ in excess, $I^-$ limited** |
|---|---|---|
| **$S_2O_3^{2-}$ limited** | $A = 0$<br>$B = b - 8a + \frac{3}{2}d > 0$<br>$C = 3a - \frac{1}{2}d > 0$<br>$D = 0$ | $A = a - \frac{1}{8}b - \frac{3}{16}d > 0$<br>$B = 0$<br>$C = \frac{3}{8}b + \frac{1}{16}d > 0$<br>$D = 0$ |
| **$S_2O_3^{2-}$ in excess** | $A = 0$<br>$B = b + a > 0$<br>$C = 0$<br>$D = d - 6a > 0$ | Unphysical, as 8 $I^-$ would give 3 $I_3^-$ which each1 $I_3^-$ would give further 3 $I^-$ thus yielding +1 net effect, that can't be limiting, if other components are there. |

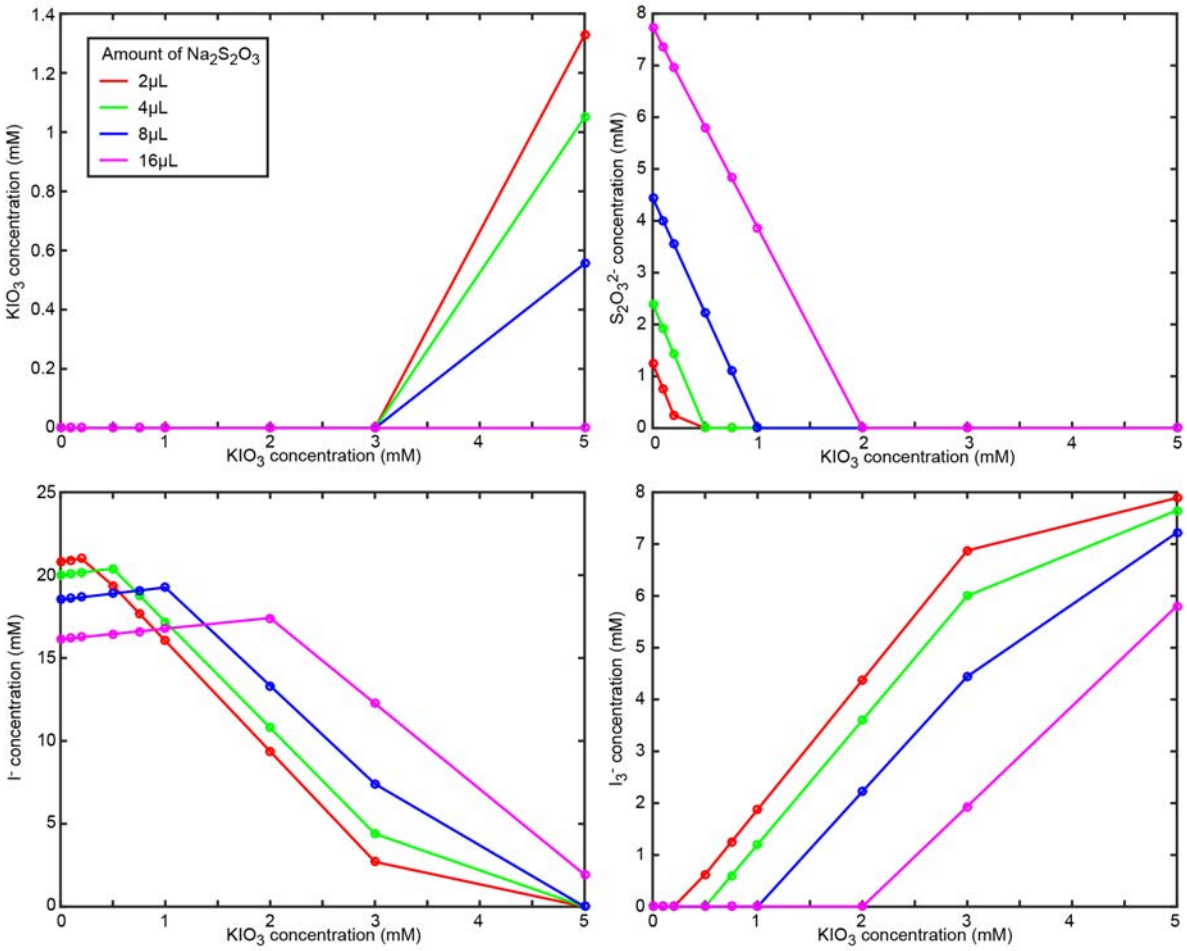


**Figure S13.** Calculated final amounts of all four compounds involved in the iodate assay reactions. All initial amounts correspond to the ones used in experiments described here.

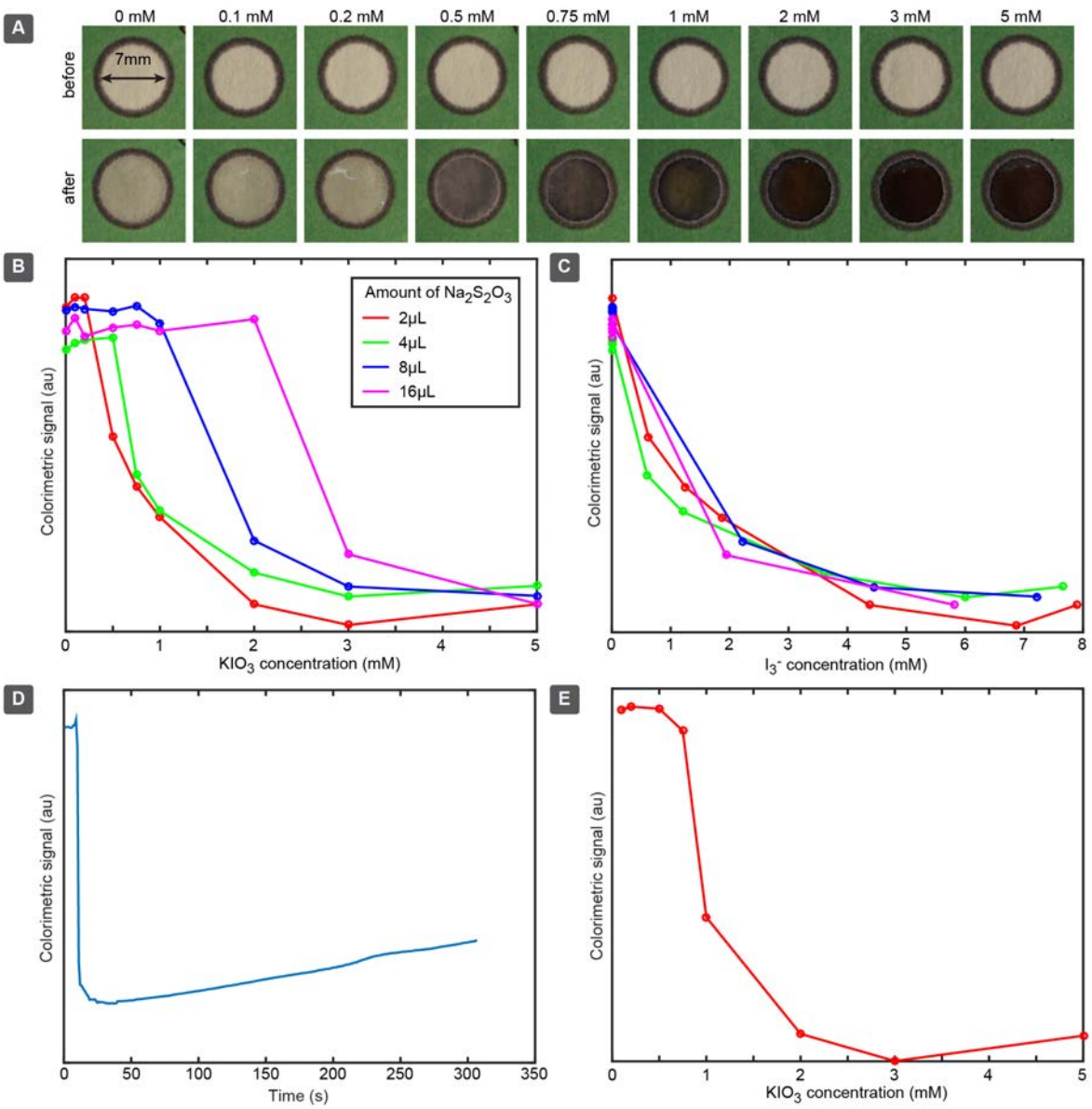


**Figure S14.** Experimental results: evaluation of starch indicator based colorimetric detection in the paper. First, the analyte and reaction components were mixed separately in test tube and product was added to the paper with starch indicator (A-D), thereafter we evaluated reaction, where components were stored in paper (E). (A) Image series of the visual appearance of the indicator area depending on analyte ($KIO_3$) concentration in the test mixture. (B) Colorimetric signal depending on analyte ($KIO_3$) concentration and amount of neutralizing $Na_2S_2O_3$. (C) Colorimetric signal depending on calculate concentration of $I_3^-$ ion, which is forming dark blue complex with starch. (D) Time dependence of the colorimetric signal. Color is the darkest (Colorimetric signal value is lowest) directly after application of the sample, but it

recovers subsequently. (E) Assay evaluation where reagents are dried and stored in the paper (amount of $Na_2S_2O_3$ is 4 μL)

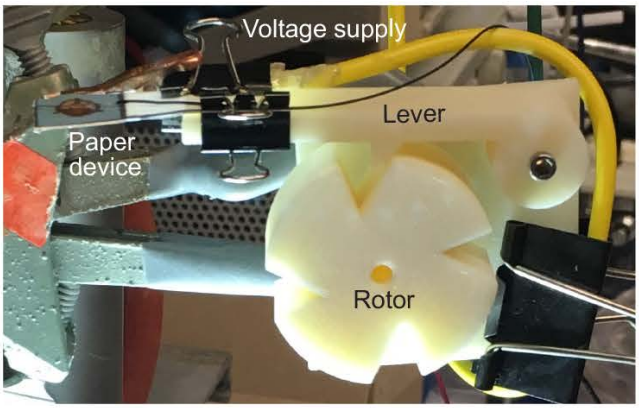


**Figure S15.** Photograph of a mechanical shaker. The rotor, lever and the assembly base were 3D printed. The rotor was driven by DC micro motor, at ~20 rpm. We used paper clips to attach the paper device and support wiring.

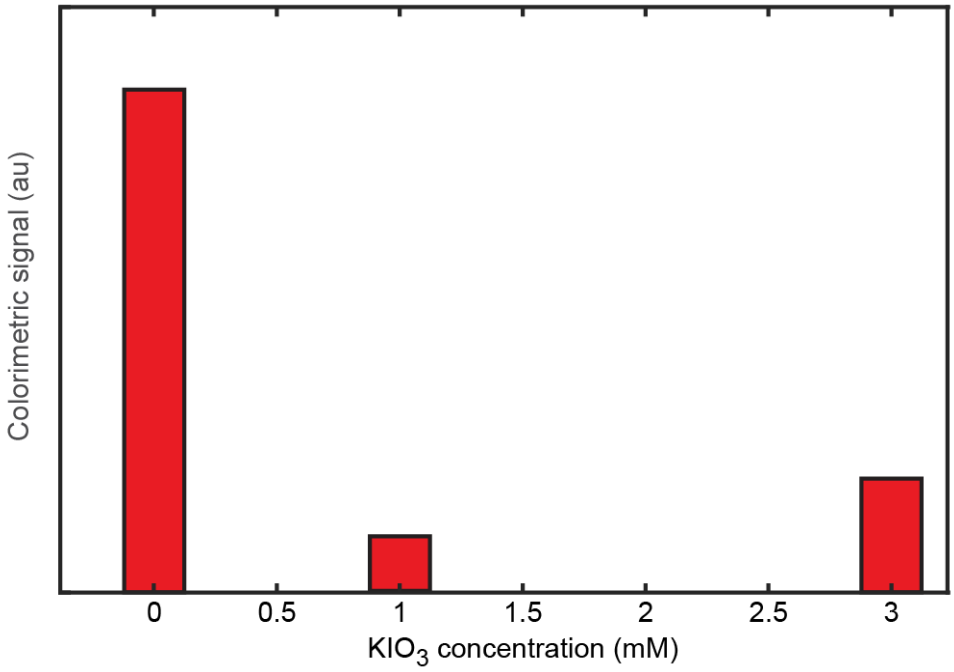


**Figure S16.** Experimental results showing colorimetric signal obtained for iodate assay with integrated valves.

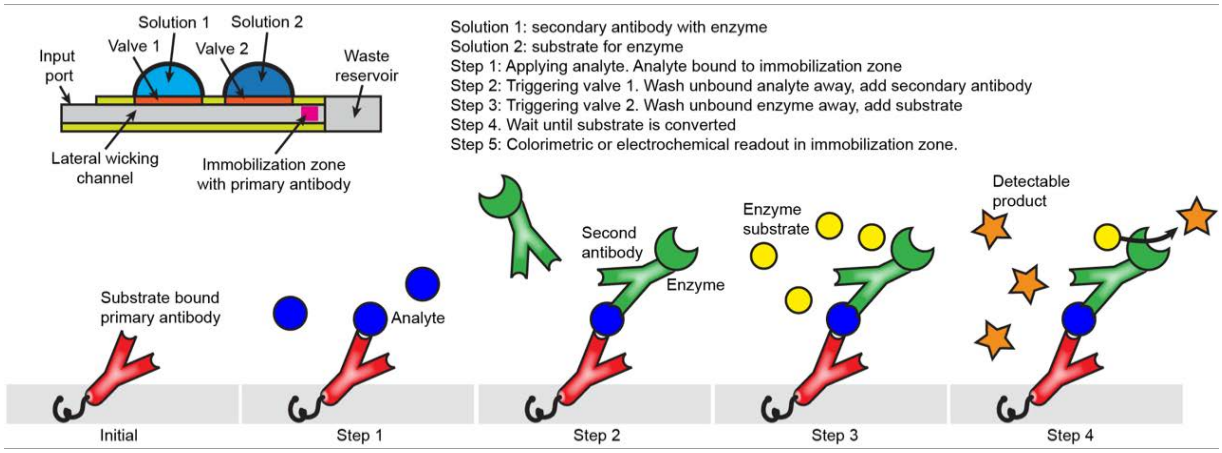


**Figure S17.** Schematic diagram showing one possible configuration that would integrate a paper-based ELISA assay in a lateral flow format, using two valves in a parallel configuration to automate the addition of reagents and the wash steps.